Analysis of the interpolation techniques for time-of-flight estimation

L. Svilainis, V. Dumbrava

Signal processing department, Kaunas University o f Technology,
Studentu str. 50, LT-51368 Kaunas, Lithuania, tel. +370 37 300532, E-mail.:svilnis@ktu.lt

Abstract
The interpolation techniques for the time-of-flight estimation have been under study. The ToF estimation was done using the direct correlation technique of the sampled signal. More accurate estimation was done using interpolation between the samples. Three interpolation techniques for discrete direct correlation are discussed: linear interpolation of zero crossing, imaginary part of direct correlation zero crossing and peak estimation using parabolic interpolation. The theoretical equations for interpolation-influenced random errors estimation have been suggested and compared with the numerical simulation. Numerical simulation allowed to analyse the influence of additional signal re-sampling on interpolation errors.
Keywords: Ultrasonic measurements, time-of-flight estimation, interpolation, acoustic signal processing.

Introduction

For decades ultrasonic systems application area is expanding: non-destructive testing and evaluation, robotic vision and navigation, measurements in production automation, medicine diagnostics and treatment, imaging in solid and liquid environments, food industry and agriculture, etc. [1-3]. One of the tasks accomplished by such systems is to define the time-of-flight (ToF) of the ultrasonic signal. In the case if the matched filter maximum likehood criterion is used for ToF estimation, the random errors produced can be evaluated using the Cramer-Rao lower bound (CRLB). [4]. Growing popularity of digital ultrasonic systems is justified by improved accuracy and adaptability of computerized processing. The digital signal processing introduces the quantization and sampling errors. The selection of proper digitization parameters is important [5]. If signal has been sampled following the Nyquist criterium, the intersample values, can be restored using the *sinc* function. But application the *sinc* interpolation is a time consuming procedure. Furthermore, in the case of the ToF measurement, only a peak position estimation is needed. Frequently, cubic spline, parabolic interpolation [6] or linear interpolation for a zero crossing in real [7] or imaginary fields [8] is used.

The analysis presented below is aimed to evaluate these techniques in a sense of sampling errors reduction in the ToF estimation procedure.

The ToF estimation

The direct correlator technique has been chosen since extensive theoretical analysis is available on the ToF estimation variance [4,6,9,10]. The technique uses position of peak of cross-corelation function R_{DC} as the ToF estimate [5]:

$$ToF_{DC} = \arg\max R_{DC}(\tau),$$
$$R_{DC}(\tau) = \int_{-\infty}^{\infty} S_T(t)\cdot S_R(t-\tau)d\tau, \quad (1)$$

where S_T is the delayed signal, S_R is the reference signal, t is the time.

The variance of ToF standard deviation when an additive white Gaussian noise (AWGN) with the power spectral density N_0 is used can be estimated as CRLB [4]:

$$std_{CRLB}(ToF) \geq \frac{1}{2\pi F_e\sqrt{\frac{2E}{N_0}}}, \quad (2)$$

where E is the signal $s_T(t)$ energy

$$E = \int_{-\infty}^{\infty} |S_T(t)|^2 dt, \quad (3)$$

F_e is the effective bandwidth of the signal:

$$F_e^2 = \frac{\int_{-\infty}^{\infty}(f-f_0)^2|S(f)|^2 df}{E} + \frac{\left[\int_{-\infty}^{\infty} f|S(f)|^2 df\right]^2}{E_2}. \quad (4)$$

Similar equations can be obtained for a digital signal [5].

The interpolation procedure

The analog signal $s(t)$ sampling can be presented as a multiplication of the analog with a delta impulse train. This will correspond to convolution in frequency domain which in turn will cause aliasing for any the frequency component falling outside the Nyquist zone $f_s/2$. Furthermore, if no interpolation is used, the ToF estimator will have some granularity defined by the sampling frequency f_s. The ToF precision will be significantly influenced by choice of the sampling frequency. Simulation results for a standard deviation of ToF estimator are presented in Fig.1.

The ultrasonic transducer with the f_c=1 MHz center frequency and 400 kHz bandwidth was used in simulation. The signal-to-noise ratio (SNR),

$$SNR = 10\lg\left(\frac{E}{N_0}\right), \quad (5)$$

was 35 dB. The resulting error can be calculated as:

$$std_{\#}(ToF) = \sqrt{std_{CRLB}(ToF)^2 + \left(\frac{1}{f_s\sqrt{12}}\right)^2}. \quad (6)$$

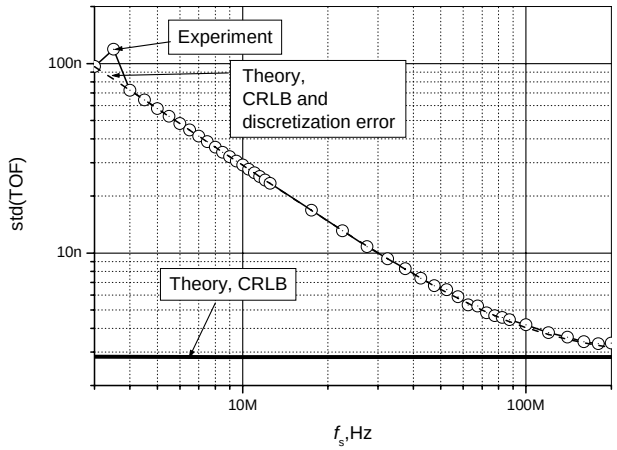

Fig 1. **ToF estimation variance when no interpolation is used**

The simulation has been carried out using MATLAB. The variance of random errors of the ToF have been obtained by taking a 1000 of runs and calculating the standard deviation of the ToF values. The noise has been simulated using *randn* function. The SNR has been varied by keeping the signal amplitude the same but changing the multiplier $\sigma_{\#}$ of *randn* function. The noise power spectral density No can be obtained from the noise waveform standard deviation $\sigma_{\#}$ and the bandwidth B ratio:

$$N_0 = \frac{\sigma_{\#}^2}{\mathrm{B}}. \qquad (7)$$

Noise bandwidth in the case of the sampled signal should be equal to the half the sampling frequency. While varying the sampling frequency, the noise power spectral density N_0 was maintained at the same level in order to assume the proper antialiasing filtering. This has been done by regulating the multiplier $\sigma_{\#}$ in the following way:

$$\sigma_{\#} = \sigma_n \sqrt{\frac{f_s}{f_{snorm}}}, \qquad (8)$$

where f_{snorm} is the sampling frequency (100 MHz) for the normalized noise level σ_n. The undersampling case was not investigated, therefore the sampling frequency starts at 3 MHz. This frequency is the first where the signal spectrum does not have significant aliasing. The aliasing effects are demonstrated in Fig.2.

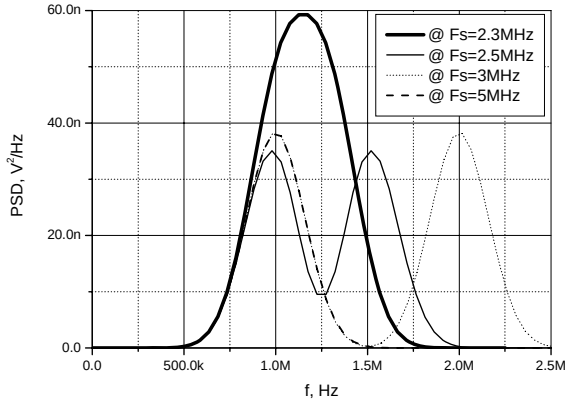

Fig 2. **Aliasing effect on the signal power spectral density (PSD) after sampling**

It can be seen that for the frequency 2.5 MHz significant aliasing occurs and for the frequency 2.3 MHz the signal spectrum is completely aliased, therefore the resulting power spectral density (PSD) is increased. This artificial increase of power in a high frequencies range is causing incorrect calculation results when using Eq. 2. This phenomenon has been reported in [5].

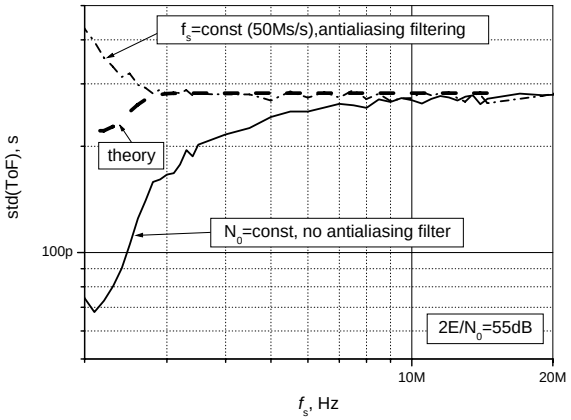

Fig. 3. **The variance of ToF for simulation**

When a proper antialiasing filter was applied, the artificial ToF variance reduction disappeared (refer Fig.3).

Increase of the sampling frequency could increase the system cost and the processing time. Therefore it is interesting to investigate the possibility to apply the interpolating function of a sparsely sampled signal in order to estimate the ToF between samples. The most accurate technique is the application of *sinc* function. But the convolution kernel for this function will be very large. In addition, we are only interested in a time domain estimation: additional samples values are not needed. Therefore it was decided to investigate the truncated *sinc* functions. Three techniques have been considered: using parabolic function for peak estimation [6], linear interpolation for zero crossing detection in a real domain [7] and zero crossing detection in an imaginary domain [8]. Parabolic interpolation application makes sense in the peak region since here it can be expected that it would be close to the *sinc* peak [5]. It is using the sample of a maximum amplitude and the two samples surrounding it (Fig.4).

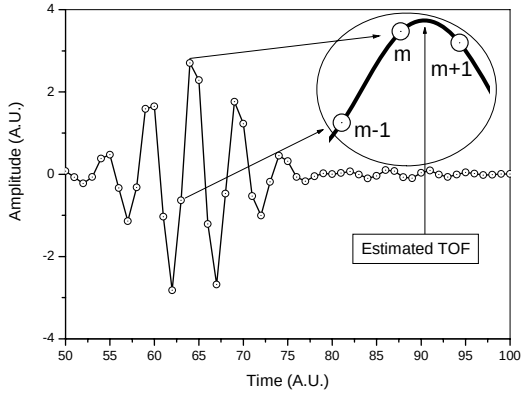

Fig. 4. **Parabolic interpolation for TOF estimation**

The positions m-1, m and m+1 obtained at the sampling period T_s are used to find the parabolic equation for apex:

$$ToF_{\#\mathrm{P}} = \frac{1}{2}\frac{(y_{m-1} - y_{m+1})T_s}{y_{m-1} - 2y_m + y_{m+1}}, \quad (9)$$

This equation can be used to calculate the additional ToF estimation errors introduced due to the noise present in sampled points. It was assumed that the T_s jitter induced by ADC is negligible compared to the influence of the noise present in sampled points m-1, m and m+1. Sensitivity coefficients for three corresponding points then are obtained as relative derivatives of the respective components:

$$s_{y1} = \frac{\partial ToF_{\#\mathrm{P}}}{\partial \mathrm{y_{m-1}}} = \frac{T_s(y_{m+1} - y_m)}{(y_{m-1} - 2y_m + y_{m+1})^2},$$
$$s_{y2} = \frac{\partial ToF_{\#\mathrm{P}}}{\partial \mathrm{y_m}} = \frac{T_s(y_{m-1} - y_{m+1})}{(y_{m-1} - 2y_m + y_{m+1})^2}, \quad (10)$$
$$s_{y3} = \frac{\partial ToF_{\#\mathrm{P}}}{\partial \mathrm{y_{m+1}}} = \frac{T_s(y_m - y_{m-1})}{(y_{m-1} - 2y_m + y_{m+1})^2}.$$

The resulting ToF estimation standard deviation is the root-mean-square (RMS) sum of the amplitude noise σ_{nDC} after direct correlation filter and the sensitivity s_{yi} coefficients product:

$$std_{\#P}(ToF) = \sqrt{\sum_{i=1}^{3}(\sigma_{nDC} \cdot s_{yt})^2} =$$
$$= T_s\sqrt{\frac{2(y_m^2 - y_m y_{m+1}^2 - y_{m+1}y_{m-1} + y_{m-1}^2 - y_{m-1}y_m)}{(y_{m-1} - 2y_m + y_{m+1})^4}}. \quad (11)$$

The results obtained using Eq. 2 and 11 are presented in Fig.5.

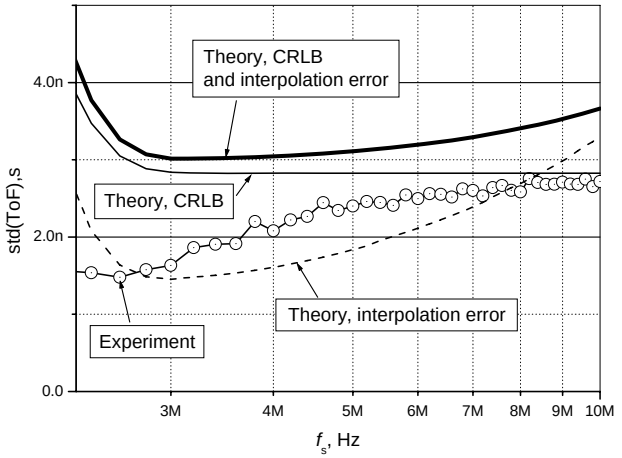

Fig. 5. **ToF estimation variance for parabolic interpolation**

Another candidate for ToF estimation is the technique, applying the low amplitudes region for a linear interpolation application of the zero crossing time instant (Fig.6).

The region of the zero crossing seems attractive since here the *sinc* function will turn into a line. The linear equation steepness coefficient b and estimation $ToF_{\#L}$ are obtained as:

$$b = -\frac{y_{z+1} + y_z}{T_s},\ ToF_{\#\mathrm{L}} = \frac{y_z T_s}{-y_{z+1} + t_z}, \quad (12)$$

from two neighboring points y_z and y_{z+1}. In the same way as per Eq. 10 and 11 the resulting ToF estimation standard deviation is obtained:

$$std_{\#\mathrm{L}}(ToF) = T_s\sqrt{\frac{2(y_{z+1}^2 + y_z^2)}{(y_z - y_{z+1})^4}}. \quad (13)$$

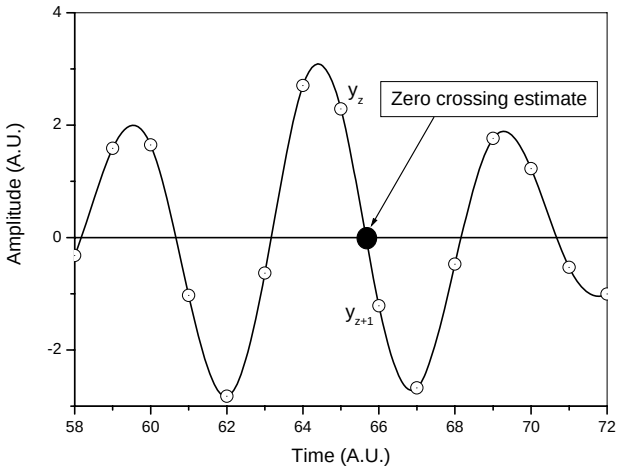

Fig. 6. **Linear interpolation of the zero crossing for TOF estimation**

The results obtained using Eq. 2 and 13 are presented in Fig.7.

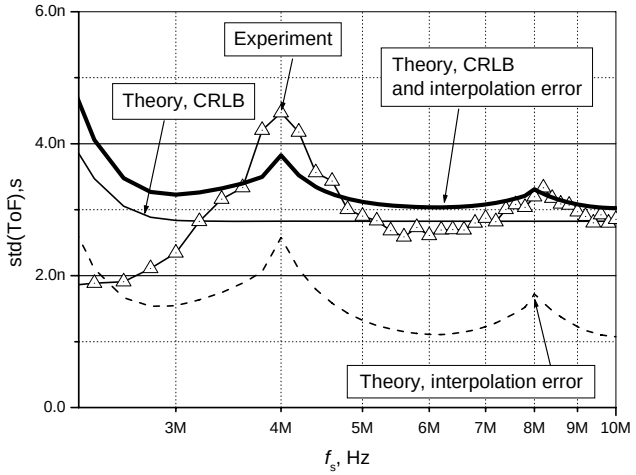

Fig. 7. **ToF variance for a linear interpolation of the zero crossing moment**

If the Hilbert transform is used to obtain the imaginary part of the correlation function [8], the zero crossing detection in the imaginary domain will correspond to the peak position. Then it seems attractive to use a linear interpolation to obtain intersample estimate of this moment. Eq. 13 will hold here. The results obtained using Eq. 2 and 13 for the zero crossing estimate and the numerical experiment results are presented in Fig.8.

In all the experiments above, the ToF variance obtained experimentally was lower than theoretical predictions. The reason was twofold: the discrepancies in estimate of the noise standard deviation after the direct correlation filter and a convenient signal placement relative to sampling points.

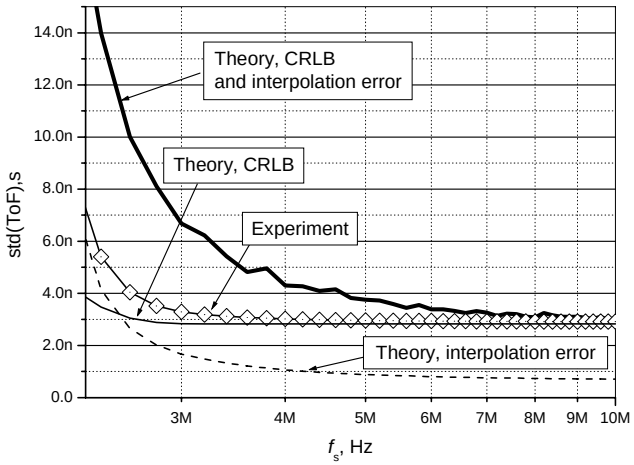

Fig. 8. **ToF estimation variance for linear interpolation of the zero crossing in the imaginary domain**

Numerical experiment for dithered time

As it was indicated in the previous chapter, ToF variance is dependant on signal placement versus sampling positions. Therefore of new numerical simulation has been carried out where the time scale dithering was introduced. Signal position in the time domain was varied along with statistics accumulation cycles. This time dither later was removed from the resulting ToF estimate, leaving statistics of all time positions influence on the ToF variance. The results for all three techniques are presented in Fig. 9.

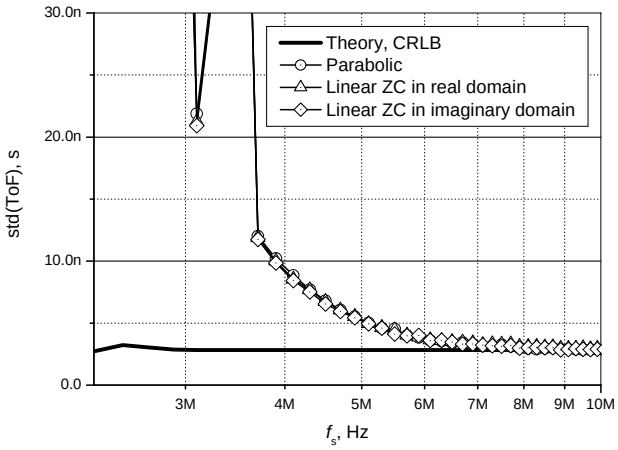

Fig. 9. **ToF variance for dithered time case**

Now it turned out that all three techniques exhibited large ToF variations in a low sampling frequency domain. One of the reasons was the increase of approximation errors, which are prevailing the random errors (Fig. 10).

Furthermore, in some cases variation was even higher (3.5 MHz point in Fig. 9). The reason here was the peak detection jumping between neighboring points since the sampling was too sparse.

Therefore it can be concluded that the sampling frequency was not sufficiently high. In order to check this assumption, the experiments were repeated with the software resampling to increase the sampling frequency 16 times (Fig. 12). The MATLAB procedure resample was used for that purpose.

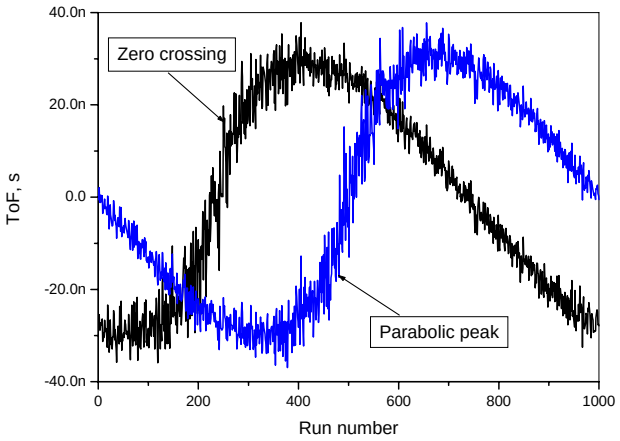

Fig. 10. **ToF values for dithered time case at 3MHz sampling**

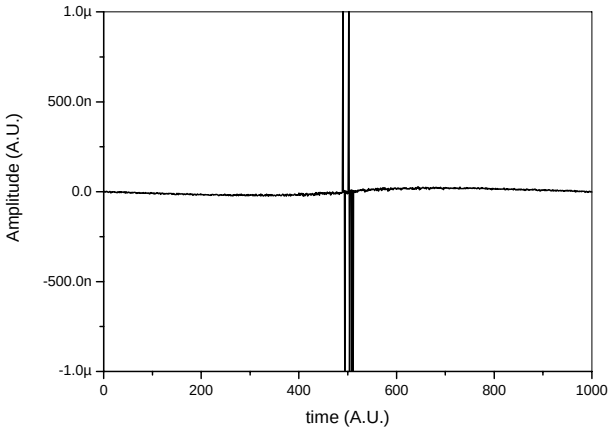

Fig. 11. **ToF jumping for the dithered time case at 3.5MHz sampling**

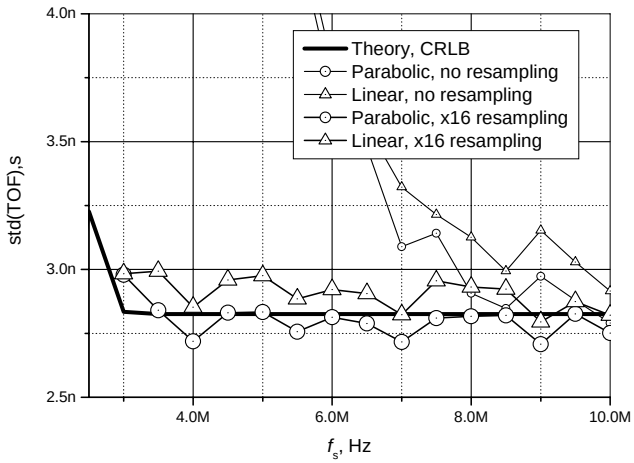

Fig. 12. **ToF variance for the dithered time case with x16 resampling**

The standard deviation of all techniques now adhered to Eq. 2 predicted values. The presented results indicate that information was present even in the data sampled at a very low frequency.

Conclusions

Investigation results indicate that a significantly low sampling frequency can be used for the high precision TOF estimation if the noise spectral density is kept constant. This should be the case if a high order antialiasing filtering is used on the received signals. Simple ToF intersample position estimation techniques, such as parabolic or linear

function fit can be used. At very low sampling frequencies these techniques have to be combined with resampling in the peak or zero crossing area. This will slow down the processing since conventional resampling procedures process the whole signal. A proper resampling procedure should be developed which is capable to apply some sort of truncated *sinc* kernel only locally in a peak area.

References

1. **Kažys R.** A review of NDT activities in Lithuania. Insight. 2001. Vol. 43(6). P.369-372.
2. **Estepar R. S. J., Stylopoulos N. et.al.** Towards scarless surgery: An endoscopic ultrasound navigation system for transgastric access procedures. Computer aided surgery. 2007. Vol.12(6). P.311-324.
3. **Tumbo S. D, Salyani M. et al.** Investigation of laser and ultrasonic ranging sensors for measurements of citrus canopy volume Applied engineering in agriculture. 2002. Vol.18(3). P.367-372.
4. **Minkoff J.** Signal processing fundamentals and applications for communications and sensing systems. Norwood, MA, USA: Artech House. 2002.
5. **Svilainis L., Dumbrava V.** The time-of-flight estimation accuracy versus digitization parameters. Ultragarsas. 2008. Vol. 63. No.1. P.12-17.
6. **Queiros R. et. al.** Cross-correlation and sine-fitting techniques for high resolution ultrasonic ranging. IMTC Instrumentation and Measurement Technology Conference. 2006. Sorento. P. 552-556.
7. **Mog G. E.; Ribeiro E. P.** Zero crossing determination by linear interpolation of sampled sinusoidal signals. Transmission and Distribution Conference and Exposition: Latin America, IEEE/PES. 2004. P.799 – 802.
8. **Kažys R.** Delay time estimation using the Hilbert transform. Matavimai. 1996. Vol.3. P.42-46.
9. **Dooley S. R., Nandi A. K.** Comparison of discrete subsample time delay estimation methods applied to narrowband signals. Measurement Science & Technology. 1998. Vol.9(9). P.1400–1408.
10. **Blok E.** Classification and evaluation of discrete subsample time delay estimation algorithms. Microwaves, Radar and Wireless Communications Conference. 2002. Vol.3. P.764 – 767.

L. Svilainis, V. Dumbrava

Interpoliacijos metodų sklidimo laikui įvertinti analizė

Reziumė

Nagrinėjami interpoliacijos metodai sklidimo laikui įvertinti skaitmeninėse ultragarsinėse sistemose. Tiesioginės koreliacijos metodas buvo naudojamas diskretizuoto signalo vėlinimo laiko įverčiui gauti. Sklidimo laikui patikslinti taikyti trys interpoliacijos metodai: nulio kirtimo tiesinė interpoliacija, pikinės vertės interpoliacija parabole ir Hilberto transformacijos būdu gautos menamosios dalies perėjimo per nulį tiesinė interpoliacija. Pasiūlytos analitinės išraiškos signalo vėlinimo laiko įverčio interpoliacijos atsitiktinėms paklaidoms įvertinti ir palygintos su skaitmeninio eksperimento rezultatais. Skaitmeniniai eksperimentai buvo skirti minėtų interpoliacijos metodų ir papildomos interpoliacijos naudojant *sinc* funkciją įtakai įvertinti.

Pateikta spaudai 2008-12-03

DOI: 10.5755/j01.u.63.4.17082